

# Quantum corrections to the ground state energy of a trapped Bose-Einstein condensate: A diffusion Monte Carlo calculation

D. Blume, and Chris H. Greene

*Department of Physics and JILA, University of Colorado, Boulder, CO 80309-0440, USA*

(October 22, 2018)

The diffusion Monte Carlo method is applied to describe a trapped atomic Bose-Einstein condensate at zero temperature, fully quantum mechanically and nonperturbatively. For low densities,  $n(0)a^3 \leq 2 \cdot 10^{-3}$  [ $n(0)$ : peak density,  $a$ :  $s$ -wave scattering length], our calculations confirm that the exact ground state energy for a sum of two-body interactions depends on only the atomic physics parameter  $a$ , and no other details of the two-body model potential. Corrections to the mean-field Gross-Pitaevskii energy range from being essentially negligible to about 20 % for  $N = 2 - 50$  particles in the trap with positive  $s$ -wave scattering length  $a = 100 - 10000$  a.u.. Our numerical calculations confirm that inclusion of an additional effective potential term in the mean-field equation, which accounts for quantum fluctuations [see e.g. E. Braaten and A. Nieto, Phys. Rev. B **56**, 14745 (1997)], leads to a greatly improved description of trapped Bose gases.

02.70.Lq, 03.75.Fi, 05.30.Jp

## I. INTRODUCTION

Since the first achievement of Bose-Einstein condensation in trapped atomic vapors in 1995 [1], these systems have received increased attention from both experimental and theoretical efforts. Theoretical studies of these inhomogeneous gases are primarily based on the mean-field Gross-Pitaevskii (GP) equation for the condensate wave function [2]. This equation can also be viewed as a variant of the Hartree-Fock (HF) approximation [3]. It is thus fundamentally important for our understanding of this many-boson system to ascertain the validity of the mean-field description and the importance of particle correlations. In principle, these questions can be investigated through the use of a complete many-body basis instead of making a single particle approximation. Some studies have in fact considered the  $T = 0$  condensate at the level of the random phase approximation (RPA), with a few going still further to treat the particle-particle correlations at the level of configuration interaction (CI) [3–6]. For many particles, however, a full CI calculation exceeds current computational capabilities. Consequently we adopt the diffusion Monte Carlo (DMC) method for the calculations reported in this paper.

In the mean-field description, the particle interactions enter solely through an effective mean-field potential, which is proportional to the  $s$ -wave scattering length

$a$  [2,7–15]. In contrast, a full description treats a many-body potential surface and allows nonseparability of the many-body wave function. The first key question of our study is therefore: Can the  $s$ -wave scattering length approximation properly describe an inhomogeneous Bose gas, or does the actual form of the two-body interaction potential necessarily come into play? To test the validity of the shape independent atom-atom potential (frequently expressed as a  $\delta$ -function potential with  $s$ -wave scattering length  $a$  [16]), we solve the  $N$ -body Schrödinger equation for an inhomogeneous Bose gas for various different two-body potentials that generate identical  $a$  using the DMC method for densities  $n(0)a^3 \leq 2 \cdot 10^{-3}$ . We find that different potentials produce indistinguishable total ground state energies  $E$ , indicating that the lowest many-body Schrödinger energy eigenvalue is independent of the shape of the two-body potential. This result is in agreement with predictions based on an expansion in  $\sqrt{n(0)a^3}$  for low densities [17,18].

However, we do observe differences between the accurate many-body ground state energy and that obtained by solving the GP equation. A second motivation of our study is therefore to assess the validity of the mean-field description as a function of  $a$  and  $N$ , and as a function of the peak density  $n(0)a^3$ . Furthermore, we test the validity of a modified GP equation that accounts for quantum fluctuations [17,19]. In addition to the ground state energy, we also show that the condensate density can be significantly affected by correlations. These calculations support our conclusion that the modified GP equation [see Eq. (3)] greatly improves upon the commonly used mean-field treatment.

Theoretical studies of correlation effects in trapped condensates have already been proposed [5,6,17–27]. These approaches include approximate zero temperature variational Monte Carlo studies [23], essentially exact finite temperature path integral Monte Carlo studies [5,6,20,21] as well as correlated basis function approaches [22], and perturbative schemes [17–19,27]. Here, we use essentially exact diffusion Monte Carlo techniques to directly calculate correlation effects at zero temperature.

Section II introduces the many-body Schrödinger equation of a trapped Bose gas and the numerical treatment applied to solve this equation. Results and their interpretation are presented in Section III. Section IV summarizes this paper.

## II. SYSTEM AND NUMERICAL TECHNIQUES

The many-body Schrödinger equation for a condensate of  $N$  mass  $m$  bosons in a spherical trap, centered at the origin with trapping frequency  $\omega_{ho}$ , is given by

$$\left( -\frac{\hbar^2}{2m} \sum_i \nabla_i^2 + \sum_{i < j}^N V(r_{ij}) + \sum_i^N \frac{1}{2} m \omega_{ho}^2 \vec{r}_i^2 \right) \psi = E \psi. \quad (1)$$

Here  $V(r_{ij}) = V(|\vec{r}_i - \vec{r}_j|)$  denotes the two-body interaction potential, and  $\vec{r}_i = (x_i, y_i, z_i)$  is the Cartesian position vector of atom  $i$  relative to the trap center.  $m$  is taken to be  $m(^{87}\text{Rb})$ , and  $\omega_{ho}$  to be  $2\pi \times 77.78$  Hz. In the following we use harmonic oscillator units for energies ( $\hbar\omega_{ho}$ ) and length ( $a_{ho} = [\hbar/(m\omega_{ho})]^{1/2}$ ). The energy per particle for the non-interacting case,  $V(r) = 0$ , is then  $E/N = 1.5 \hbar\omega_{ho}$ , and, for example, the  $^{87}\text{Rb}$   $s$ -wave triplet scattering length ( $a \approx 100$  a.u.),  $a = 0.00433 a_{ho}$  at that frequency.

The DMC method [28] (and references therein), here implemented with importance sampling and a descendant weighting scheme, derives a solution to the many-body ground state Schrödinger equation, Eq. (1), for a given model potential surface. This solution is essentially exact, apart from statistical uncertainties. The resulting ground state energy shall be denoted by  $E_{DMC}$  in the following. Ideally, one would solve Eq. (1) for the best known  $^{87}\text{Rb}$ - $^{87}\text{Rb}$  two-body potential  $V(r)$  (e.g. Ref. [29]). However, the large number of bound states in this potential makes its use in a many-body calculation extremely challenging, if not infeasible (see below). Instead, we have carried out tests using three different two-body model potentials A-C to test how the energetics depend on the actual form of the two-body potential: A) a purely repulsive hard core potential with hard core radius  $a$ ,  $V(r) = \infty$  for  $r < a$  and  $V(r) = 0$  for  $r \geq a$ ; B) another purely repulsive potential with parameters  $d > 0$  and  $r_0$ , namely  $V(r) = d \cosh^{-2}(r/r_0)$ ; and C) a sum of an attractive and a repulsive Gaussian, leading to a potential that exhibits a minimum with negative energy. The potential parameters are adjusted such that *i*)  $a = 0.00433 a_{ho}$  (potentials A-C), and *ii*)  $a = 0.433 a_{ho}$  (potentials A and B).

Potential C requires a few more remarks. In contrast to potentials A and B, which are purely repulsive, potential C is repulsive at short range and attractive at long range. The usage of this potential in a DMC calculation could therefore potentially lead to a lowest energy state that describes a cluster rather than a condensed state. However, the two-body potential is such that it does not support a two-body bound state; nevertheless, many-body bound states might exist. If this two-body potential supports a many-body bound state, then our simulation should converge to a cluster state rather than to the metastable condensed state at infinite imaginary

simulation time. At finite time, however, we find empirically for positive  $a$  that our DMC simulation samples the condensed and not the cluster state.

To test our DMC code we carry out a separate exact solution to Eq. (1) for two particles,  $N = 2$ , by separating out the center of mass motion and solving the one-dimensional radial Schrödinger equation using standard numerical techniques. For potential A we find, for example,  $E = 3.00345 \hbar\omega_{ho}$  for  $a = 0.00433 a_{ho}$ , and  $E = 3.3827 \hbar\omega_{ho}$  for  $a = 0.433 a_{ho}$  in excellent agreement with our DMC results,  $E_{DMC} = 3.00346(1) \hbar\omega_{ho}$  and  $E_{DMC} = 3.3831(7) \hbar\omega_{ho}$ , respectively. (The statistical error of the DMC energies is given in parenthesis.) Since the DMC algorithm generalizes straightforwardly as a function of  $N$ , the above agreement is a convincing test of our code. Furthermore, we carefully checked the independence of our results on the exact shape of the trial wave function and on the time step used for the propagation in imaginary time. The next section presents results from our DMC calculation and compares them with GP theory.

## III. RESULTS AND INTERPRETATION

Columns 2-4 of Table I show the DMC energies  $E_{DMC}$  for  $N = 3 - 20$  for the three two-body potentials A, B and C with *i*)  $a = 0.00433 a_{ho}$  (top) and *ii*)  $a = 0.433 a_{ho}$  (bottom). For the parameter range considered in Table I, which corresponds to  $n(0)a^3 \leq 2 \cdot 10^{-3}$  (see below), the ground state energy  $E_{DMC}$  of the inhomogeneous gas for different  $V(r)$  with identical two-body scattering length  $a$  is independent of the shape of  $V(r)$ ; and thus  $E_{DMC}$  depends only on  $a$  to within our statistical uncertainties. For the homogeneous Bose gas, Giorgini *et al.* [30] find a small dependence of the ground state energy on the shape of the two-body potential in the intermediate density regime,  $na^3 \approx 10^{-3}$  ( $n$ : number density of homogeneous gas); however, their energy depends only on  $a$  in the low density regime. Recent extensive studies of trapped two- and three-particle condensates as a function of the scattering length  $a$  and the trap frequency  $\omega_{ho}$  reveal dependences of the ground and excited state energies on the exact shape of the two-body potential in the high density limit. However, these studies will be presented elsewhere.

To ascertain the validity of the widely used mean-field approach, we now compare our many-body DMC energies with those obtained by solving the GP equation,

$$\left[ \frac{-\hbar^2}{2m} \nabla^2 + \frac{1}{2} m \omega_{ho}^2 \vec{r}^2 + \frac{4\pi\hbar^2(N-1)a}{m} |\Phi_{GP}(\vec{r})|^2 \right] \times \Phi_{GP}(\vec{r}) = \epsilon_{GP} \Phi_{GP}(\vec{r}). \quad (2)$$

Here,  $\Phi_{GP}(\vec{r})$  denotes the ground state orbital (normalized to 1), and  $\epsilon_{GP}$  the orbital energy; the total energy  $E_{GP}$  can be obtained through evaluation of the energy

functional  $E_{GP}[\Phi_{GP}]$  [2]. Notice that  $\epsilon_{GP}$  can also be associated with the chemical potential of the system. Both  $\epsilon_{GP}$  and  $E_{GP}$  depend only on  $(N-1)a$ , rather than on  $a$  and  $N$  separately. The formulation of the GP equation in terms of  $(N-1)a$  rather than  $Na$  follows from number conserving Schrödinger quantum mechanics, using a HF initial state [3]. To compare our DMC energies  $E_{DMC}$  with the GP energies  $E_{GP}$ , our many-body DMC calculations reported below have been performed for potential A only, which is the purely repulsive hard core potential. Since  $E_{DMC}$  is independent of the shape of  $V(r)$  (see Table I), this justifies our restriction to only one two-body potential. Note, however, that our calculations reported in the following treat densities  $n(0)a^3$  as large as  $\approx 1$ . In this high density regime we expect the many-body energy to depend on the detailed shape of the two-body potential.

Figure 1(a) compares the ground state energies  $E_{GP}$  and  $E_{DMC}$  for  $N = 2 - 50$  as a function of the interaction parameter  $(N-1)a/a_{ho}$  [Eq. (2)]. Note the logarithmic scale for  $(N-1)a/a_{ho}$ ; diamonds and triangles show our calculated data points, while solid and dotted lines connect those data points with identical  $N$  but different  $a$ . The full quantum energies  $E_{DMC}$  are always equal to or larger than the mean-field energies  $E_{GP}$ , with  $(E_{DMC} - E_{GP})/E_{DMC}$  attaining 20 to 50 % for the largest scattering lengths  $a$  considered here,  $a = 3.9, 3.0, 2.6, 1.7, 0.87, 0.43 a_{ho}$  for  $N = 2, 3, 5, 10, 20, 50$ . Figure 1(a) shows the separate dependences of  $E_{DMC}$  on  $a$  and  $N$ ; e.g., for  $(N-1)a = 10 a_{ho}$ ,  $(E_{DMC} - E_{GP})/E_{DMC} \approx 0.4$  for  $N = 5$ , but instead  $\approx 0.07$  for  $N = 50$ . Column 5 of Table I summarizes  $E_{GP}$  for a few selected  $N$  and  $a$  parameters. In conclusion, the GP equation, Eq. (2), describes the condensate accurately for small  $a$ . For larger  $a$ , however, significant departures occur from the DMC results. Later in this section we discuss these departures further.

We refer to the energy difference  $E_{DMC} - E_{GP}$  as a “correlation energy”  $E_{corr}$ . Note that the definition of  $E_{corr}$  introduced here differs from that often used in quantum chemistry, where  $E_{corr}$  is defined as the energy difference between the CI energy  $E_{CI}$  and the HF energy  $E_{HF}$  for the same two-body potential  $V(r)$ . In our treatment  $E_{DMC}$  results from solving the many-body Schrödinger equation, Eq. (1), for the exact wave function (= complete basis) with a *shape dependent* two-body potential  $V(r)$ , whereas  $E_{GP}$  results from the mean-field equation, Eq. (2), or equivalently, from Eq. (1) for a *shape independent*  $\delta$ -function potential using a HF initial state. Thus,  $E_{corr}$  not only contains basis set effects, but also effects due to the reduction of the shape dependent interaction potential to a shape independent potential that generates an identical scattering length  $a$ . Note that  $E_{DMC} \geq E_{GP}$ , and therefore  $E_{corr} \geq 0$ , for the parameter range considered here. The “exact” many-body treatment of the particle interaction (using a model two-body potential) leads evidently to an *increase* of the mean-field energy  $E_{GP}$ , which is somewhat coun-

terintuitive. Recent calculations for potentials of type B with negative potential depth  $d$  show, however, that the many-body energy can be lower than the GP energy for extremely tight traps,  $\nu_{ho} \approx 10$  MHz (see, e.g., Fig. 3 of [4]). In the following we restrict ourselves to the hard core potential A.

Next, we assess a modified GP equation, which has been discussed in the literature [17,18]. Braaten and Nieto [17] included the effects of quantum fluctuations for positive  $a$  to generate corrections to the mean-field equation. Qualitatively, quantum fluctuations can be viewed as representing virtual double excitations of particles out of the condensate, which is also related to the ground state depletion. Within the Thomas-Fermi (TF) approximation, these “quantum corrections” produce an additional local effective potential term in the GP equation that is linear in the assumed small parameter  $(na^3)^{1/2}$ ,

$$\left[ \frac{-\hbar^2}{2m} \nabla^2 + \frac{1}{2} m \omega_{ho}^2 \vec{r}^2 + \frac{4\pi\hbar^2(N-1)a}{m} |\Phi_{GP,mod}(\vec{r})|^2 \right. \\ \left. \times \left( 1 + \frac{32}{3\sqrt{\pi}} a^{\frac{3}{2}} (N-1)^{\frac{1}{2}} \Phi_{GP,mod}(\vec{r}) \right) \right] \Phi_{GP,mod}(\vec{r}) = \epsilon_{GP,mod} \Phi_{GP,mod}(\vec{r}). \quad (3)$$

The total energy  $E_{GP,mod}$  relevant to this modified GP equation can be obtained from the energy functional  $E_{GP,mod}[\Phi_{GP,mod}]$ . Equation (3) accounts for two-body physics through the scattering length  $a$  solely; three-body effects are not included. In contrast to Eq. (2), which only depends on the interaction parameter  $(N-1)a$ , Eq. (3) exhibits separate dependences on  $N-1$  and  $a$ . Note that inclusion of second order terms in the TF expansion leads to additional non-local terms in Eq. (3), which account for edge effects [17]. Our estimates suggest that these non-local terms are small, and we have therefore neglected them.

The term accounting for quantum fluctuations for the inhomogeneous gas, the second term in the second line of Eq. (3), is identical to the Huang-Lee-Yang correction term for the homogeneous gas [11–13]. Huang, Lee and Yang showed in 1957 that the many-body Schrödinger equation for a Bose gas interacting via hard sphere potentials can be equivalently formulated by replacing the hard sphere boundary conditions by a pseudo-potential. This pseudo-potential can then be treated in perturbation theory, leading to a lowest order ground state energy per particle  $E_0/N \approx 2\pi\hbar^2(a/m)n$ . To next order in  $(na^3)^{1/2}$ , the first order perturbation energy can be evaluated by summing over momentum states with wave vector  $\vec{k} \neq 0$  [13], resulting in  $E_0/N \approx 2\pi\hbar^2(a/m)n[1 + \frac{128}{15\sqrt{\pi}}(na^3)^{1/2}]$  for the homogeneous gas. The summation over  $\vec{k}$  states depends crucially on use of the exact pseudo-potential expansion: Use of  $4\pi\hbar^2(a/m)\delta(\vec{r})$  rather than  $4\pi\hbar^2(a/m)\delta(\vec{r})\frac{\partial}{\partial r}r$  leads to a divergent ground state energy expression. The additional term arising in first order perturbation theory for the homogeneous gas is identical to the term in the

inhomogeneous gas accounting for quantum fluctuations (using quantum mean-field theory language) [17], and directly shows the contribution of  $k \neq 0$  (excited) states to the ground state energy. Braaten and Nieto [17] stress that the most important excitations are to orbitals in the energy range  $E_{excitation} \approx 8\pi\hbar^2(a/m)n$ .

The derivation of Eq. (3) is based on two assumptions [17]: *i*) the expansion parameter  $(na^3)^{1/2}$  is small, and *ii*)  $1/\sqrt{na}$  is small compared to the condensate radius. To assess the accuracy of these assumptions explicitly, Fig. 1(b) compares  $E_{GP,mod}$  obtained from Eq. (3) with our DMC energy  $E_{DMC}$ . Consider the  $N = 2$  curve first.  $E_{DMC} - E_{GP,mod}$  is positive for small  $a$ , switches sign at  $a \approx 0.2 a_{ho}$ , reaches its minimum for  $a \approx 0.87 a_{ho}$ , and becomes positive for  $a > 1.7 a_{ho}$ . The behavior for larger  $N$  is similar. The maximal negative deviation for the parameter range shown in Fig. 1(b) is about 3 % for  $N = 5$  and  $a \approx 0.87 a_{ho}$ . For  $N = 20$  and  $N = 50$ , the agreement between  $E_{DMC}$  and  $E_{GP,mod}$  is better than 3 % for  $a$  as large as  $0.87 a_{ho}$  ( $\approx 20000$  a.u.) for  $N = 20$ , and  $0.43 a_{ho}$  ( $\approx 10000$  a.u.) for  $N = 50$ , respectively. Table I summarizes  $E_{GP,mod}$  for a few selected values of  $N$  and  $a$ .

The modified GP equation, Eq. (3), overcorrects the correlation effects for some  $a$  for all  $N$  considered. Overall, the additional effective potential term in Eq. (3) improves the GP treatment substantially for  $N = 2-50$ . As the size of the condensate increases, we expect the next higher order correction terms, which are non-local [17], to become even smaller, and the local correction term considered in Eq. (3) to be the dominant one. It should be noted, however, that Eq. (3) is derived in the large  $N$  regime, where the number of particles contributing to quantum fluctuations is small compared to those occupying the “single particle ground state” [17]. Thus the excellent agreement between  $E_{GP,mod}$  and  $E_{DMC}$  in the small  $N$  limit might be somewhat fortuitous.

Figure 2 shows the same data as in Fig. 1(a), however, now as a function of  $(N-1)(a/a_{ho})^3$  rather than the interaction parameter  $(N-1)a/a_{ho}$ . All data points,  $N = 2-50$ , lie on a “universal curve”. As we shall discuss later, this universal behavior suggests that our calculations for small  $N$  and their comparison with mean-field and quantum mean-field treatment may directly transfer to inhomogeneous gases with larger  $N$ .

To summarize our ground state energy studies, note the different scales of the vertical axes in Figs. 1(a) and (b). A comparison of (a) and (b) shows that a significant improvement over GP theory is accomplished through the inclusion of quantum fluctuations [Eq. (3)], as evidenced by the better agreement between  $E_{GP,mod}$  and  $E_{DMC}$  than between  $E_{GP}$  and  $E_{DMC}$ .

Besides the ground state energy, we also calculate structural properties using Eqs. (1)-(3). The peak density  $n(0)$ , for example, determines many properties such as the lifetime of a trapped condensate, and its exact determination is therefore of great importance. Figure 3 summarizes our results for the radial density per parti-

cle  $n(r)/N$  for  $N = 3$  (a) and  $N = 10$  (b) for two different scattering lengths  $a$ , where  $\int n(r)d^3\vec{r} = N$ . Our DMC density per particle  $n_{DMC}(r)/N$  [Eq. (1)] is shown as triangles for  $a = 0.0433 a_{ho}$  and as diamonds for  $a = 0.433 a_{ho}$ . Note that these data points have statistical noise. Dashed lines indicate the GP density per particle  $n_{GP}(r)/N$  [Eq. (2)], while dotted lines show the modified GP density per particle  $n_{GP,mod}(r)/N$  [Eq. (3)]. For the smaller scattering length,  $a = 0.0433 a_{ho}$ , all three densities per particle,  $n_{DMC}(r)/N$ ,  $n_{GP}(r)/N$  and  $n_{GP,mod}(r)/N$ , agree well. In fact, for  $N = 3$  the modified GP density and the GP density are indistinguishable. For the larger scattering length,  $a = 0.433 a_{ho}$ ,  $n_{GP,mod}(r)/N$  coincides with the DMC density  $n_{DMC}(r)/N$ , whereas the GP equation overestimates the peak density by about 20 % ( $N = 3$ ), and 35 % ( $N = 10$ ), respectively. For comparison, the GP treatment underestimates the energy for this scattering length by only 4 % (10 %), whereas the modified GP equation overestimates the energy by only about 2 % (2 %) for  $N = 3$  ( $N = 10$ ).

The calculation of the DMC density  $n_{DMC}(r)$ , and especially the peak density  $n_{DMC}(0)$ , is more time intensive than that of the DMC energy  $E_{DMC}$ . To replot our data from Fig. 2 we therefore approximate  $n_{DMC}(0)$  by  $n_{GP,mod}(0)$ , which is easy to calculate. Figure 4 shows the fractional energy correction  $(E_{DMC} - E_{GP})/E_{DMC}$  on a log-log scale as a function of  $n_{GP,mod}(0)a^3$  for  $10^{-4} \leq n_{GP,mod}(0)a^3 \leq 1$  (solid and dotted lines). In addition, the dashed line shows the fractional correction to the GP energy predicted within quantum mean-field theory using the TF (large  $N$ ) limit,  $x/(1+x)$ , where  $x = 7/8\sqrt{\pi n(0)a^3}$  [2,17,18]. The larger  $N$ , the smaller the difference between the fractional correction to the GP energy based on our DMC calculation for small  $N$  and the asymptotic large  $N$  limit (dashed curve). Figure 4 seems to suggest that the predicted behavior based on quantum mean-field theory within the TF limit [2,17,18] is indeed correct, and gives an accurate estimate of the error of the GP equation as a function of the density  $n(0)a^3$  for large  $N$ . Our calculations may therefore be viewed as a first explicit numerical test of the application of quantum mean-field theory to trapped Bose gases.

#### IV. SUMMARY

This paper presents full quantum calculations for an inhomogeneous Bose gas that serve as a stringent test of mean-field theory. Our calculations suggest that condensates are well described through only the  $s$ -wave scattering length  $a$ . Other characteristics of the two-body potential such as the effective range parameter seem to be negligible for the  $a$  and  $N$  parameter range considered here. These findings for the inhomogeneous gas are in agreement with quantum mean-field predictions [17,19,18], and recent DMC studies for the homogeneous Bose gas [30]. Our studies also suggest that the

first order correction term [Eq. (3)] leads to a great improvement upon the GP equation, [Eq. (2)], for large  $a$ . For a spherical trap with, for example,  $N = 5000$  particles and  $a = 0.0433 a_{ho}$  (1000 a.u.) the GP and the modified GP energies differ noticeably, at the 5.9 % level:  $E_{GP}/N = 9.239 \hbar\omega_{ho}$ , and  $E_{GP,mod}/N = 9.786 \hbar\omega_{ho}$ . The densities for this condensate differ at the 15 % level:  $n_{GP}(0)a^3 = 1.9 \cdot 10^{-3}$  and  $n_{GP,mod}(0)a^3 = 1.7 \cdot 10^{-3}$ . We expect the excitation frequencies to change by an amount comparable to that of the energy [31,32]. Very recently, stable condensates with large scattering length  $a = 10000$  a.u., corresponding to a density  $n(0)a^3 = 10^{-2}$ , have been obtained experimentally in a non-spherical trap [33].

The studies presented here are performed for a two-body potential with positive scattering length  $a$ , which supports no two-body bound state. It will be interesting to extend these studies to two-body potentials with negative  $a$ . Furthermore, the interplay between recombined molecular (i.e. “snow flake”) and BEC-type states, completely neglected in this work, promises rich physics.

## V. ACKNOWLEDGEMENTS

This work was supported partly by the National Science Foundation. D. B. acknowledges support through a DFG Postdoktorandenstipendium. Extensive discussions with John L. Bohn, E. Braaten and B. D. Esry have been greatly appreciated.

- [15] A. L. Fetter and J. D. Walecka, Quantum theory of many-particle systems, McGraw-Hill, New York (1971).
- [16] E. Fermi, Nuovo Cimento **11**, 157 (1934).
- [17] E. Braaten and A. Nieto, Phys. Rev. B **56**, 14745 (1997).
- [18] E. Timmermans, P. Tommasini and K. Huang, Phys. Rev. A **55**, 3645 (1997).
- [19] J. O. Anderson and E. Braaten, Phys. Rev. A **60**, 2330 (1999).
- [20] W. Krauth, Phys. Rev. Lett. **77**, 3695 (1996).
- [21] P. Grüter, D. Ceperley and F. Laloë, Phys. Rev. Lett. **79**, 3549 (1997).
- [22] A. Fabrocini and A. Polls, Phys. Rev. A **60**, 2319 (1999).
- [23] J. L. DuBois and H. R. Glyde, cond-mat/0008368 (unpublished).
- [24] M. A. Zahuska-Kotur, M. Gajda, A. Orłowski and J. Mostowski, Phys. Rev. A **61**, 033613 (2000).
- [25] K. Ziegler and A. Shukla, Phys. Rev. A **56**, 1438 (1997).
- [26] D. A. W. Hutchinson, R. J. Dodd and K. Burnett, Phys. Rev. Lett. **81**, 2198 (1998).
- [27] S. A. Morgan, J. Phys. B: At. Mol. Opt. Phys. **33**, 3847 (2000).
- [28] B. L. Hammond, W. A. Lester, Jr. and P. J. Reynolds, Monte Carlo Methods in Ab Initio Quantum Chemistry, (World Scientific, Singapore, 1994).
- [29] M. Krauss and W. J. Stevens, J. Chem. Phys. **93**, 4236 (1990).
- [30] S. Giorgini, J. Boronat and J. Casulleras, Phys. Rev. A **60**, 5129 (1999).
- [31] L. Pitaevskii and S. Stringari, Phys. Rev. Lett. **81**, 4541 (1998).
- [32] E. Braaten and J. Pearson, Phys. Rev. Lett. **82**, 255 (1999).
- [33] S. L. Cornish, N. R. Claussen, J. L. Roberts, E. A. Cornell and C. E. Wieman, Phys. Rev. Lett. **85**, 1795 (2000).

- 
- [1] M. H. Anderson, J. R. Ensher, M. R. Matthews, C. E. Wieman and E. A. Cornell, Science **269**, 198 (1995).
  - [2] F. Dalfovo, S. Giorgini, L. P. Pitaevskii and S. Stringari, Rev. Mod. Phys. **71**, 463 (1999).
  - [3] B. D. Esry, Phys. Rev. A **55**, 1147 (1997).
  - [4] B. D. Esry and C. H. Greene, Phys. Rev. A **60**, 1451 (1999).
  - [5] M. Holzmann, W. Krauth and M. Naraschewski, Phys. Rev. A **59**, 2956 (1999).
  - [6] M. Holzmann and Y. Castin, Eur. Phys. J. D **7**, 425 (1999).
  - [7] N. Bogolubov, J. Phys. (Moscow) **11**, 23 (1947).
  - [8] L. P. Pitaevskii, J. Exptl. Theoret. Phys. **40**, 646 (1996) [Sov. Phys. JETP **13**, 451 (1961)].
  - [9] E. P. Gross, Nuovo Cimento **20**, 454 (1961).
  - [10] E. P. Gross, J. Math. Phys. **4**, 195 (1963).
  - [11] K. Huang and C. N. Yang, Phys. Rev. **105**, 767 (1957).
  - [12] T. D. Lee and C. N. Yang, Phys. Rev. **105**, 1119 (1957).
  - [13] T. D. Lee, K. Huang and C. N. Yang, Phys. Rev. **106**, 1135 (1957).
  - [14] K. Huang, Statistical mechanics, John Wiley and Sons, New York (1963).

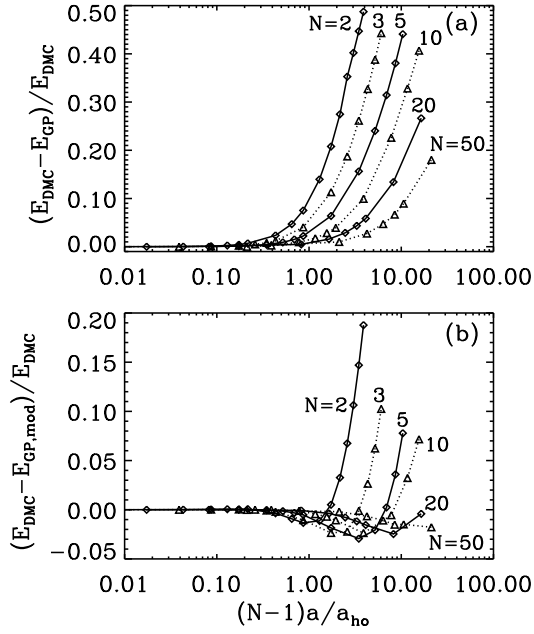


FIG. 1. Energy difference  $E_{DMC} - E_{GP}$  normalized by  $E_{DMC}$  (a) and  $E_{DMC} - E_{GP,mod}$  normalized by  $E_{DMC}$  (b), respectively, as a function of the GP interaction parameter  $(N-1)a/a_{ho}$ . Diamonds and triangles show data points resulting from solving Eqs. (1)-(3), and solid and dotted lines connect data points for identical  $N$  to guide the eye,  $N = 2 - 50$ . Note the logarithmic  $(N-1)a/a_{ho}$  scale.

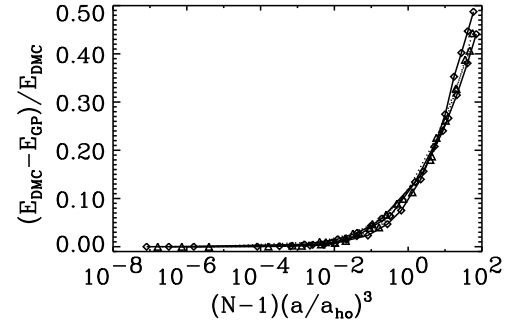


FIG. 2. Energy difference  $E_{DMC} - E_{GP}$  normalized by  $E_{DMC}$ , also shown in Fig. 1(a), however, now as a function of  $(N-1)(a/a_{ho})^3$  rather than the interaction parameter  $(N-1)a/a_{ho}$ . All data points,  $N = 2 - 50$ , line up on a “universal curve”. Note the logarithmic  $(N-1)(a/a_{ho})^3$  scale.

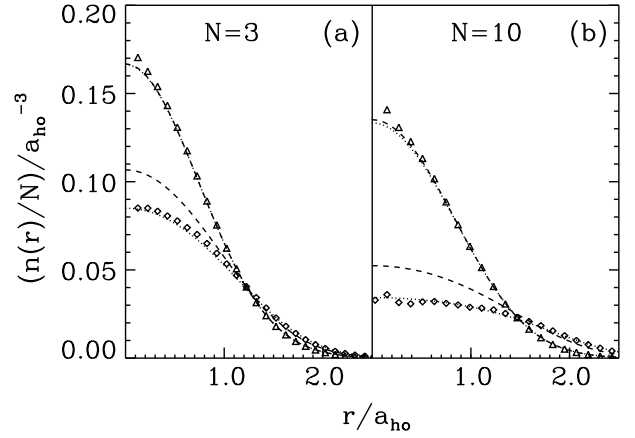


FIG. 3. DMC density per particle  $n_{DMC}(r)/N$  together with GP density per particle  $n_{GP}(r)/N$  and the modified GP density per particle  $n_{GP,mod}(r)/N$  for  $N = 3$  (a) and  $N = 10$  (b) for two different scattering lengths  $a$ . Triangles show the DMC density for  $a = 0.0433 a_{ho}$ , diamonds that for  $a = 0.433 a_{ho}$ . Dashed lines show the GP and dotted lines the modified GP densities per particle. The statistical error of the DMC data is smaller than the size of the symbols at large  $r$ , and about twice the size of the symbols near the trap center (small  $r$ ). Note  $n_{GP}(r)/N$  and  $n_{GP,mod}(r)/N$  are indistinguishable on the scale shown for  $N = 3$  and  $a = 0.0433 a_{ho}$ .

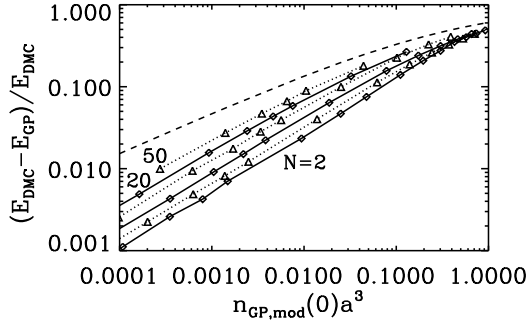


FIG. 4. Energy difference  $E_{DMC} - E_{GP}$  normalized by  $E_{DMC}$ , also shown in Fig. 1(a) and 2, however, now as a function of  $n_{GP,mod}(0)a^3$  (solid and dotted lines) for densities  $10^{-4} \leq n_{GP,mod}(0)a^3 \leq 1$  together with the fractional correction to the GP energy calculated within quantum mean-field theory using the TF approximation (dashed line, see text). Note the logarithmic scale of both axes.

$N$	potential A	potential B	potential C	$E_{GP}$	$E_{GP,mod}$
3	4.51036(2)	4.51037(2)	4.51035(4)	4.51032	4.51032
5	7.53443(4)	7.53439(6)	7.53441(10)	7.53432	7.53434
10	15.1537(2)	15.1539(2)	15.1536(8)	15.1534	15.1535
20	30.640(1)	30.639(1)	30.638(2)	30.638	30.639
3	5.553(3)	5.552(2)		5.329	5.611
5	10.577(2)	10.574(4)		9.901	10.772
10	26.22(8)	26.20(8)		23.61	26.84
20	66.9(4)	66.9(1)		57.9	68.5

TABLE I. Ground state energies  $E_{DMC}$ , columns 2-4, in units of  $\hbar\omega_{ho}$  for three different two-body potentials A-C for  $N = 3 - 20$  particles in the trap; top for  $a = 0.00433 a_{ho}$  (potentials A-C), and bottom for  $a = 0.433 a_{ho}$  (potentials A-B). The statistical uncertainty is given in parenthesis. For comparison columns 5 and 6 contain the GP energy  $E_{GP}$  and the modified GP energy  $E_{GP,mod}$ , respectively.